Mofiz, S.A. and Rahman, M.M. (2010) Evaluation of failure load-deformation characteristics of geo-reinforced soil using simplified approach. Auckland, New Zealand: 11th IAEG Congress, 5-10 Sep 2010. 4383-4392.

Evaluation of failure load-deformation characteristics of geo-reinforced soil using simplified approach

S.A. Mofiz
Department of Civil Engineering, Rajshahi University of Engineering & Technology, Bangladesh
M.M. Rahman
Department of Civil and Natural Resources Engineering, University Canterbury, New Zealand

ABSTRACT: In this research work, a comprehensive testing program has been carried out to study the stress-strain and volume change behavior of unreinforced and reinforced residual soil. A series of drained triaxial tests were conducted using computer controlled GDS triaxial apparatus for unreinforced and reinforced soil. Test results show that reinforced soils exhibit higher failure strains and volume contraction than unreinforced soils. Reinforced soils with non-woven geotextile exhibit higher failure strains, strength and coefficient of interface friction than woven geotextile reinforced residual soil. A simplified approach for numerical calculations were proposed to predict the shear strength of unreinforced and reinforced soils for triaxial compression stress paths and the coefficient of interface friction for reinforced soils. Charts were also presented to predict the strength of reinforced soil and to determine the coefficient of interface friction from triaxial tests. Predictions of failure stress using simplified approach are satisfactory compared to laboratory observations.

1 Introduction

The strains in the soils due to a given increment of stress vary considerably depending on the stress-level and confining pressure. In the field, soil elements undergo different stress paths depending upon the loading condition. Reinforced soil has gained popularity due to its extensive application in various problems such as retaining walls, pavements, foundations, embankments, etc. These problems are often analysed by finite element method. The non-linear stress-strain relationship, which may be highly dependent on the confining stress, was formulated and implemented for finite element analysis by Ling and Tatsuoka (1992). Ling and Tatsuoka (1994) conducted a study on silty clay reinforced with three types of geosynthetics, two geotextiles, and a geogrid under plane strain conditions. Taha et al. (1999) demonstrated the behaviour of georeinforced residual soil using drained triaxial samples, shown that the reinforced systems increased strength-deformation properties in a significant manner. Ashmawy et al. (1999) reported that reinforced soils exhibit an improvement in strength-deformation characteristics under monotonic loading conditions, due to the additional “pseudo” confinement caused by the lateral restraint and shear mobilization. The present research works is aimed to determine the stress-strain mechanism between the reinforcement and soil using stress path tests. However, with respect to residual soil, both its interaction mechanism and its failure behaviour in soil composites are not well understood due to limited study. Thus, a thorough investigation of the soil reinforcement interaction was conducted. The simplified prediction procedures to determine the strength of reinforced and unreinforced soils for various stress paths were presented. An attempt was undertaken to determine the coefficient of interface friction from test results. Prediction charts have been presented for different friction angle of soil and number of reinforcement layers.

2 PROPERTIES OF SOIL AND REINFORCEMENT

Residual soils often found in tropical or semi-tropical area, are formed from intense weathering of rocks under consistently high temperature and rainfall. In this work, the disturbed soil was collected from the barind area of Bangladesh. The soil is reddish in colour and classified as CH in the Unified

Classification System (USCS). The soil contains about 50% clay, 20% silt, 30% sand and no gravels. The maximum dry density from the standard Proctor test was 14.42 kN/m$_3$ and the optimum moisture content was about 23.6%. In this research work, a non-woven geotextile was used as the reinforcement material. This group of geotextiles consists of mechanically bonded continuous filaments made from UV-stabilized polypropylene. The tensile strength properties of the reinforcement were determined following ASTM D4595 (ASTM 2000). The maximum tensile strength from the tests was obtained 17.68 kN/m and 19.12 kN/m in the longitudinal and transverse direction, and the corresponding elongations were about 70%, 52% respectively.

3 TEST PROCEDURE

In this investigation, twelve consolidated drained triaxial stress path tests were performed on the unreinforced residual soil as shown in Figure 1. The six stress path tests were followed using 50 mm diameter and 100 mm high cylindrical triaxial specimen for both unreinforced and reinforced soil. Based on the unit weight and the volume of the triaxial mold, the total weight of the soil was divided into three equal portions and compacted inside the mold in layers of equal height. For reinforced specimen, two circular discs of non-woven geotextile were placed at the 1/3 height from the top and 1/3 height from the bottom of the specimens. A rate of 0.15 mm/min for compression on a triaxial press was adopted, and each layer was compacted following the approach by Cui and Delage (1996) to ensure Proctor maximum density with a double piston system. The tests reported in this paper for both unreinforced and reinforced soil were carried out under consolidation pressure in the range 100–600 kPa. A strain rate of 0.0015%/min was used to ensure no pore pressure change as required in a drained test. The computer controlled triaxial (GDS) system was adapted to carry out all the stress path tests. A microprocessor collects the data from transducers automatically at prescribed intervals. The data were transmitted by the controlling microprocessor for recording, processing and production of results, which could be displayed on the screen.

4 TEST RESULTS

For compression and extension stress path test, the stress-strain and volume change plots for the different stress paths at a consolidation pressure σ_c = 100 kPa are presented

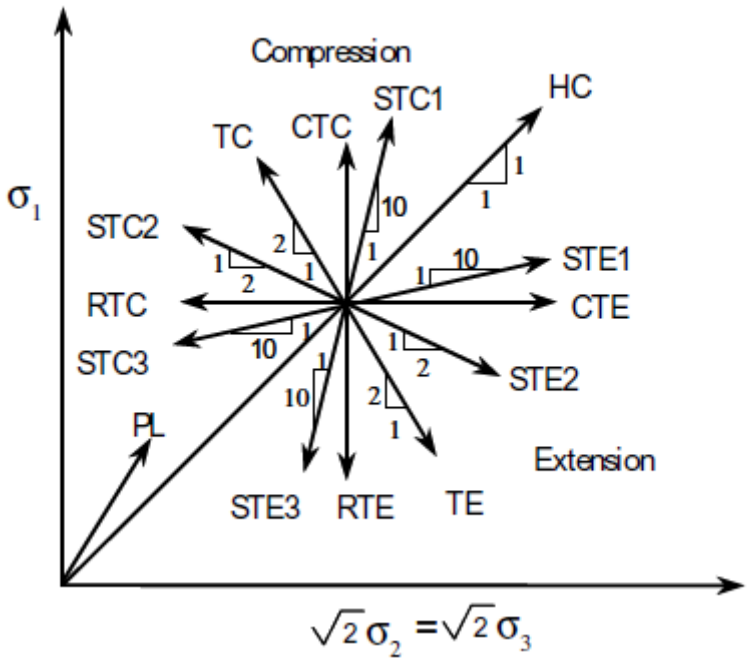

Figure 1. Schematic representation of the different stress paths on triaxial plane.

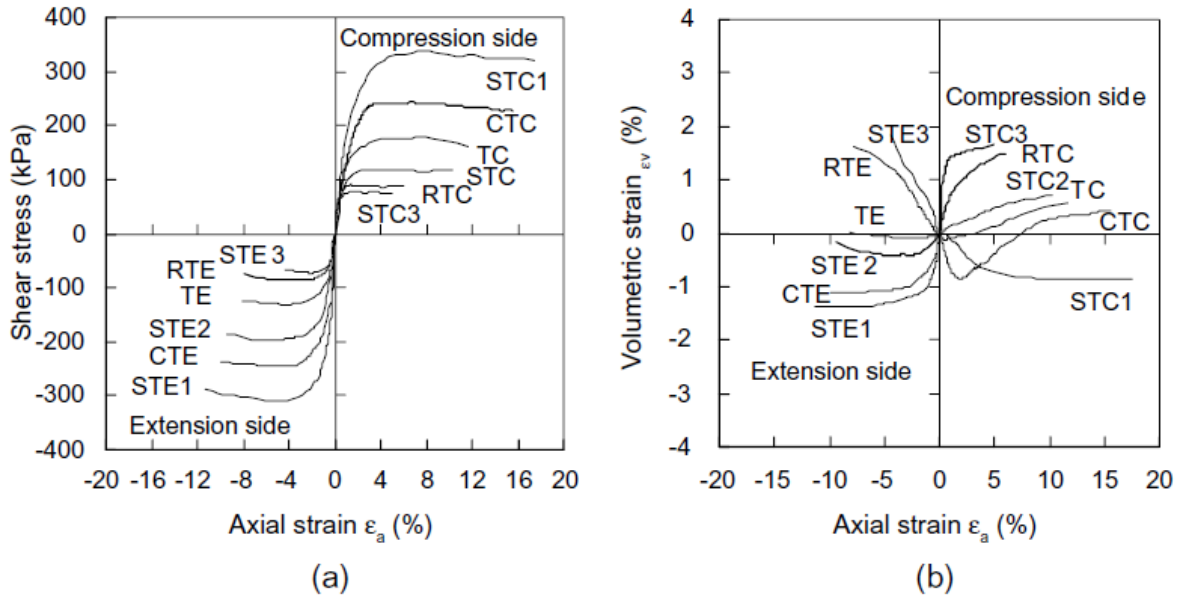

Figure 2. Behaviour of soil at consolidation pressure (∫c = 100 kPa) for different stress paths: (a) shear stress vs. axial strain (b) volumetric strain vs. axial strain.

Figure 2(a) and 2(b). In the compression stress path, failure strains (∑ₐ) are maximum for STC1 stress path and minimum for STC3. At low stress levels the volume change characteristics exhibits volume contraction for STC1 and CTC stress path whereas expansions for STC2 and STC3 stress path. As one moves from STC1 path to STC3 path, the volume change contraction decreases and the soil starts expansion even at low stress levels. This phenomenon is most likely due to decreasing confining pressure and dependent on the stress path followed. In the extension side, the negative failure strain (□∑ₐ) is maximum in STE1 stress path and minimum for STE3 stress paths. Test observations of STE1 and CTE paths indicate that the volume contraction is higher due to the gradual increase of cell pressure. The volume contraction decreases from STE2 to TE whereas expansion behaviour was observed for RTE and STE3 paths. This contraction-expansion behaviour is the result of the gradual decrease of axial stress and incremental increase of confining pressure. In this research, it is observed that the cohesion intercept and the angle of internal friction of the residual soil for the compression stress path are higher than that for the extension stress path. This is possibly the mobilised shear strength is higher due to the soil particles try to reconsolidate under compression loading. For the extension path, it has slightly lower values because the shear load is applied in the lateral or reverse direction which may cause soil to fail under tensile forces. The failure envelopes of unreinforced soil in terms of s2 = (∫2₁ + ∫2₃)/2, t = (∫₁ – ∫₃)/2 for the compression and extension stress paths are presented in Figure 3a and Figure 3b. Test results show that the shear strength parameters are slightly different in compression and extension loadings. The cohesion and angle of internal friction of unreinforced soil under compression and extension loading are c2 = 27.42 kPa, \2 = 28.02° and c2 = 23.50 kPa, \2 = 27.00° respectively. However, in each side, the parameters are independent of the stress path.

As expected, the non-woven geotextiles reinforced samples exhibit higher shear strength than unreinforced samples and the maximum shear strength were attained at higher axial strains. This increase of shear strength is caused by an increase of the confining pressure in the soil between the reinforcement layers which depends on the interface friction resistance along the reinforcement. The shear strength parameters for a two layered non-woven geotextile reinforced soils are determined from the MIT stress path method. The cohesion intercept and angle of internal friction for a two layered reinforced soil under compression and extension loading are c2 = 43.85 kPa, \2 = 32.4° and c2 = 38.56 kPa, \2 = 30.81° as shown in Figure 4. It is also observed that the reinforced soils exhibit higher failure strain and shows about 20% to 43% higher than that of unreinforced soils. The failure

strains also increases with the increase of reinforcement layers. Comparison of strength parameters and failure strains for unreinforced and reinforced soil are presented in Table 1 and Table 2.

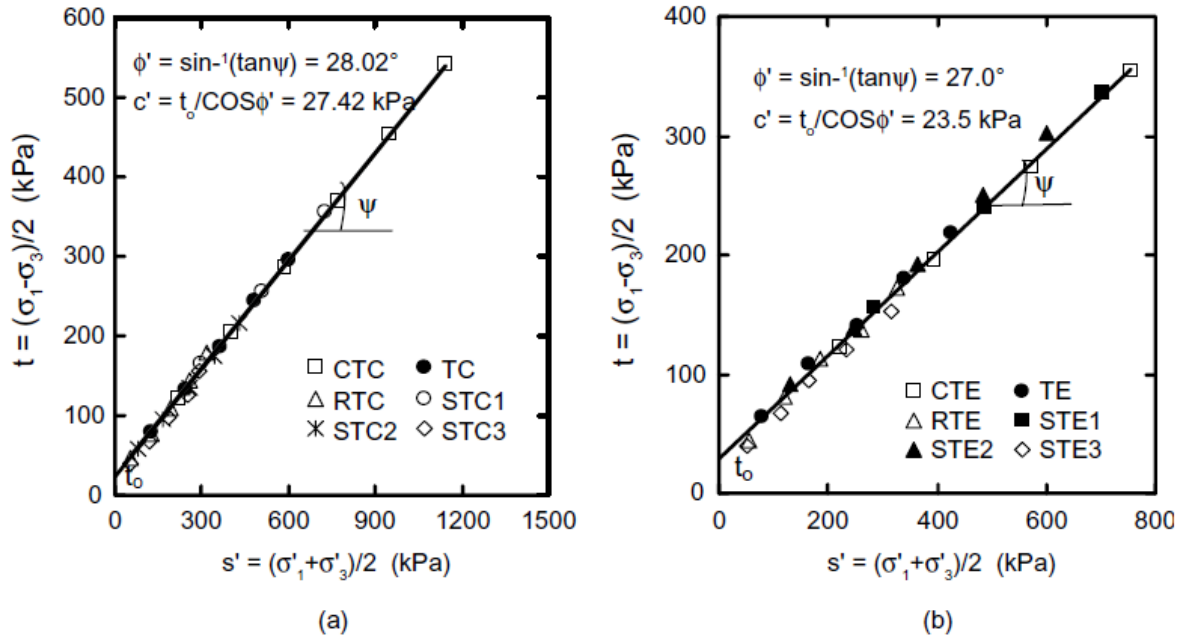

Figure 3. MIT failure envelopes for unreinforced residual soil: (a) compression stress paths (b) extension stress paths.

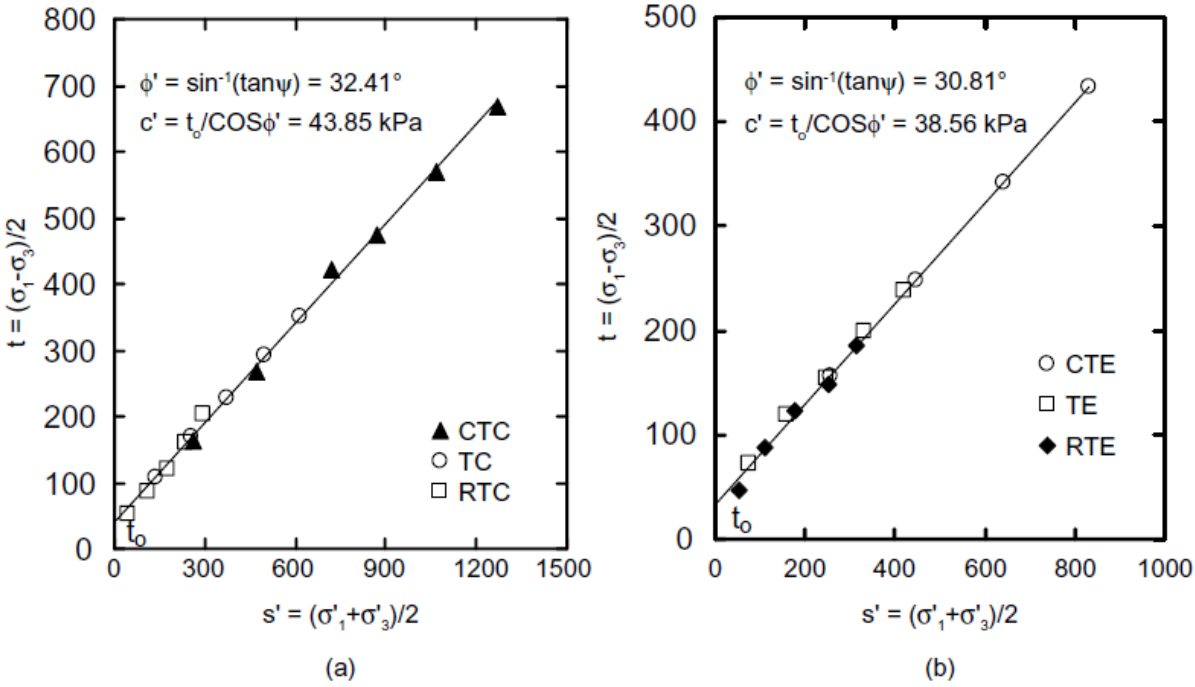

Figure 4. MIT failure envelopes for a two layered non-woven geotextile reinforced soil: (a) compression stress path (b) extension stress path.

Table 1. Comparison of strength parameters for unreinforced and reinforced soil.

Types of specimen	Stress path	Cohesion, c' (kPa)	Friction angle, ϕ'°	Increase of parameters over unreinforced soil	
				c'	ϕ'°
Unreinforced	Compression	27.42	28.02	–	–
	Extension	23.50	27.00	–	–
Reinforced	Compression	43.85	32.41	16.43	4.39
	Extension	38.56	30.81	15.06	3.81

Table 2. Comparison of failure strains of unreinforced and reinforced soil at consolidation pressure $\sigma_c = 100$ kPa.

Stress paths	Failure strain of unreinforced soil (%)	Failure strains of reinforced soil (%)	Increase of failure strains over unreinforced soil (%)
CTC	7.91	11.33	43.23
TC	7.15	9.69	35.52
RTC	3.84	5.18	34.89
CTE	5.96	8.22	37.92
TE	4.95	6.87	38.78
RTE	3.82	5.08	32.98

5 ELASTIC PARAMETERS

Elastic parameters can be used to evaluate the stress-strain properties or the elastic and volumetric response of soils. The initial tangent modulus and modulus of elasticity for various compression stress paths can be determined using the above relationships. Similar procedure follows for another stress paths in compression and extension. The initial tangent modulus relationships for the different stress paths on compression and extension loadings are presented in Table 3.

The non-linear elastic model parameters for unreinforced and reinforced residual soil are then determined for the various stress paths. The elastic parameters are obtained following the procedures outlined by Duncan et al. (1980). Boscardin et al. (1990) also followed the same procedure to determine the elastic and bulk modulus for soil composites. The plots of Ei/Pa (Pa = atmospheric pressure) and σ3/Pa on log-log scale for compression and extension stress paths are shown in Figure 5 and Figure 6. From the results, it is observed that the initial tangent modulus is maximum for triaxial compression (STC3) and minimum for triaxial compression (STC1). For extension stress paths, the test results showed higher initial tangent modulus in STE1 stress path and lower value for STE3 stress path. It can be concluded that the elastic parameters are also dependent on the stress paths. The elastic constants of unreinforced and reinforced soil for compression and extension stress paths are presented in Table 4 and Table 5.

For compression path, the result illustrates that the modulus and exponent number shows highest values in STC3 and lowest in STC1 paths. Similarly, in extension, the variation of modulus and exponent number is such that it shows the highest under STE1 and lowest values under STE3 paths. This follows the values of the failure strains and also dependent on the loading conditions (stress

path). It is also observed that there is no significant variation of the failure ratio (Rf) for both compression and extension.

6 PREDICTION OF SHEAR STRENGTH BY SIMPLIFIED APPROACH

The prediction of the shear strength of reinforced soils depends on different factors such as the tensile strength of the reinforcement, confining pressure, number of reinforcement layer and interface friction. Yang (1972) reported for the first time the concept of increase in confining pressure due to insertion of reinforcement. Broms (1977) and Chandrasekaran et al. (1989) proposed various expressions for the shear strength of reinforced soil considering Yang's concept.

For reinforced soil, the axial stress, σ_1, can be expressed as

$$\sigma_1 = \frac{\sigma_3 N_\phi + 2c'\sqrt{N_\phi}}{1 - \dfrac{f\,d\,K_{av}}{2\,h\,K_a}}$$

For single layer reinforced soil, the axial stress, σ_1 can be predicted from Equation 1 if the values of f, d, h, σ_3 and γ2 are known.

Table 3. Initial tangent modulus relationships for various stress paths.

Test loading condition	Types of stress path	Initial tangent modulus E_i (kPa)	Modulus of elasticity E (kPa)
Compression	STC1	9E/(2(5 – ν))	(2/9)(5 – ν)E_i
	CTC	E	E_i
	TC	3E/(2(1+ν))	2Ei/3(1+ν)
	STC2	3E/(4(0.25+ν))	(4/3)(0.25+ν)E_i
	RTC	E/2ν	2νE_i
	STC3	–9E/(10(0.1 – ν))	(–10/9)(0.1 – ν)E_i
Extension	STE1	9E/(2(5 – ν))	(2/9)(5 – ν)E_i
	CTE	E	E_i
	STE2	3E/(4(0.25+ν))	(4/3)(0.25+ν)E_i
	TE	3E/(2(1+ν))	2Ei(1/3(1+ν))
	RTE	E/2ν	2νE_i
	STE3	–9E/(10(0.1 – ν))	(–10/9)(0.1 – ν)E_i

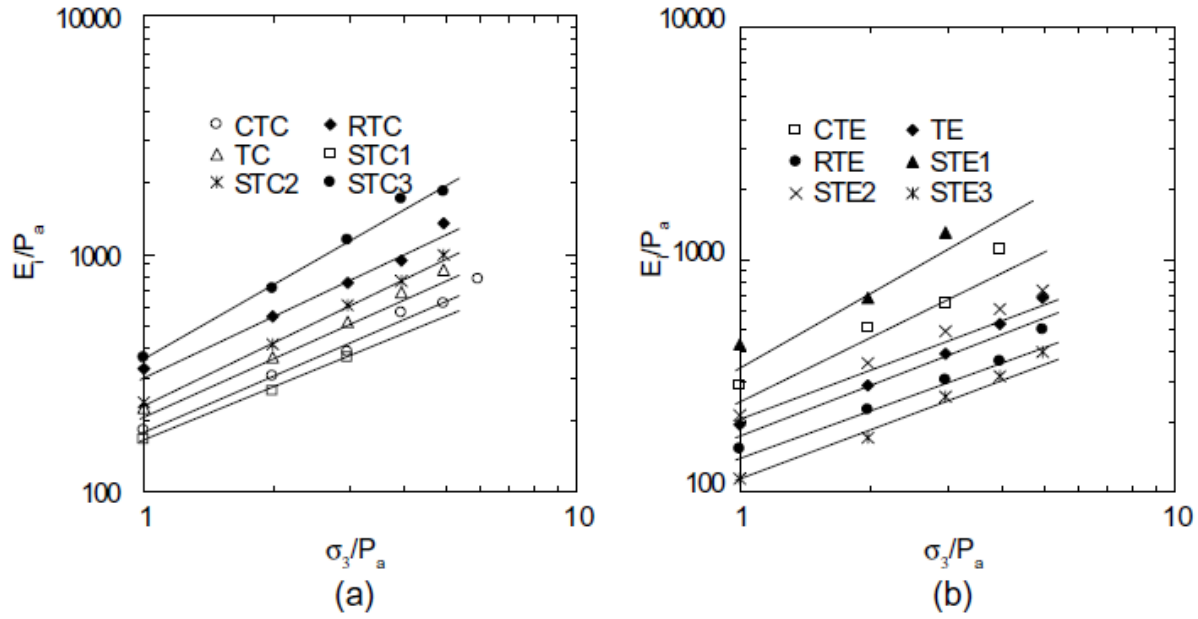

Figure 5. Representation of elastic parameters for unreinforced soil: (a) compression stress path

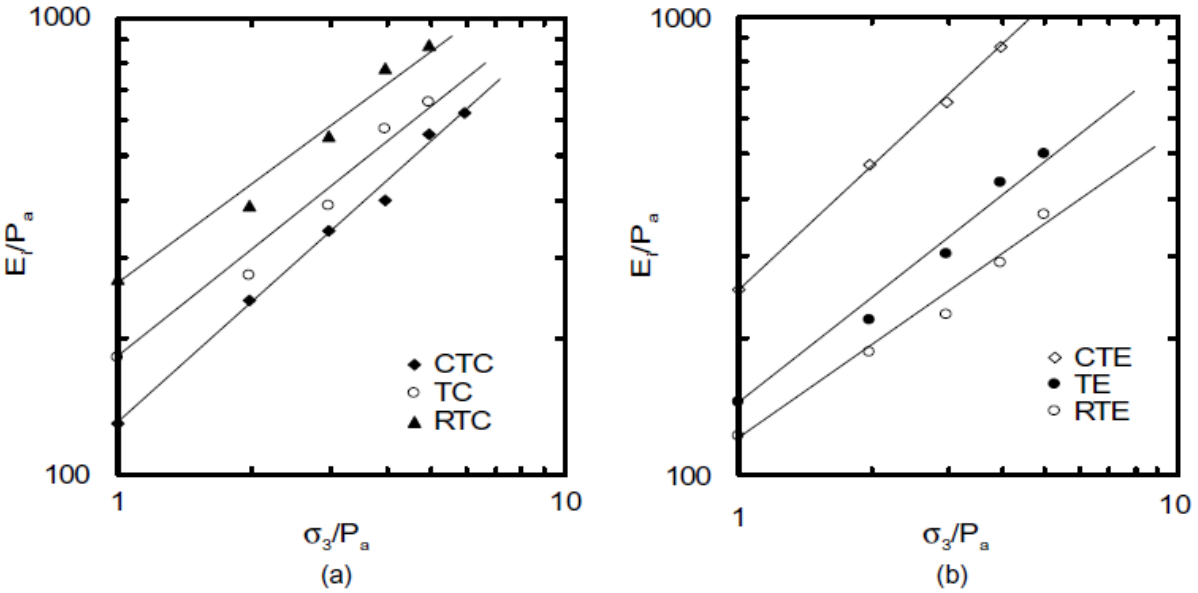

Figure 6. Representation of elastic parameters for a two layered non-woven geotextile reinforced soil: (a) compression stress path (b) extension stress path.

Table 4. Elastic constants of unreinforced soil for various stress paths.

Test loading condition	Type of stress paths	Confining pressure (kPa)	Elastic parameters		
			K	n	R_f
Compression	CTC	100 to 600	181	0.82	0.81
	TC	100 to 500	225	0.83	0.83
	RTC	100 to 500	315	0.89	0.84
	STC1	100 to 300	168	0.71	0.86
	STC2	100 to 500	235	0.89	0.84
	STC3	100 to 500	369	0.99	0.90
Extension	CTE	100 to 400	250	0.97	0.85
	TE	100 to 500	170	0.79	0.84
	RTE	100 to 500	151	0.74	0.85
	STE1	100 to 300	405	1.01	0.92
	STE2	100 to 500	214	0.77	0.84
	STE3	100 to 500	115	0.78	0.81

Table 5. Elastic constants of a two layered non-woven geotextile reinforced soil for various stress paths.

Test loading condition	Types of stress path	Confining pressure (kPa)	Elastic parameters		
			K	n	R_f
Compression	CTC	100 to 600	130	0.87	0.76
	TC	100 to 500	172	0.80	0.85
	RTC	100 to 500	262	0.73	0.88
Extension	CTE	100 to 400	252	0.88	0.86
	TE	100 to 500	134	0.77	0.84
	RTE	100 to 500	116	0.69	0.85

A general expression for the axial stress in terms of *N* layers of reinforcement can be written as

$$\sigma_1 = \frac{\sigma_3 N_\phi + 2c'\sqrt{N_\phi}}{1 - \dfrac{f\, d\, K_{av}}{2h K_a} \displaystyle\sum_1^N \left(1 - \frac{2s}{h}\right)}$$

Equation 2 indicates that the shear strength of reinforced soil is a function of σ_3, $\phi 2$, *f*, *N*, (s/h) and (d/h). The coefficient of interface friction has been determined using the failure stress at consolidation pressures σ_c = 200 kPa and σ_c = 400 kPa for CTC path only. Back predictions of the failure axial stress were then calculated using the average coefficient of friction for the various stress paths. The axial stress of reinforced soil with reinforcement inclusions for various stress paths is calculated using Equation 2. Comparisons were made with the experimental results as shown in Table 6. The result shows that the predicted response is a good agreement with the experimental values.

7 PREDICTION OF THE COEFFICIENT OF INTERFACE FRICTION

The coefficient of interface friction of the reinforced soil can determined either from the pull out test or the modified direct shear test. In the field, the reinforced soil is normally subjected to a confining

stress. Thus, conducting triaxial tests at the required confining pressure can simulate such conditions. Therefore, an attempt is made to determine the coefficient of

Table 6. Measured and predicted axial stress at failure for CTE and TC stress path.

Stress paths	No. of layers	Friction coeff. f	Friction angle, ϕ	Cons.stress σ_c, (kPa)	Axial stress σ_1, (kPa)	
					Measured	Predicted
CTE	2	0.34	27°	100	411	398
				200	695	681
				300	982	984
				400	1266	1287
TC	2	0.34	28.02°	100	245	241
				200	424	421
				300	605	610
				400	791	800

interface friction from the triaxial test results. The coefficient of interface friction, *f*, can be determined by using any stress path test from the values of axial stress at failure, confining stress, angle of internal friction of unreinforced soil, number of reinforcement layers, (s/h) and (d/h), respectively. It is very convenient to determine the coefficient of interface friction, f, by conducting the conventional triaxial compression (CTC) stress path tests. In this stress path the value of f can be determined by rearranging Equation 2.

$$f = \frac{\frac{K_a}{K_{av}}\left[1-\left(\frac{\sigma_3}{\sigma_1}\right)\tan^2(45+\phi'/2)-\frac{2c'\sqrt{\tan^2(45+\phi'/2)}}{\sigma_1}\right]}{\left[\left(\frac{d}{2h}\right)\sum_1^N\left(1-\frac{2s}{h}\right)\right]}$$

For single layer horizontal reinforcement placing at the centre of the specimen, the coefficient of interface friction can be determined as

$$f = \frac{\frac{K_a}{K_{av}}\left[1-\left(\frac{\sigma_3}{\sigma_1}\right)\tan^2(45+\phi'/2)-\frac{2c'\sqrt{\tan^2(45+\phi'/2)}}{\sigma_1}\right]}{\left(\frac{d}{2h}\right)}$$

The above equation can be rewritten when the reinforcement is placed at the mid height of the specimen (d/h = 0.5)

$$f = \frac{4K_a}{K_{av}}\left[1-\left(\frac{\sigma_3}{\sigma_1}\right)\tan^2(45+\phi'/2)-\frac{2c'\sqrt{\tan^2(45+\phi'/2}}{\sigma_1}\right]$$

The coefficient of interface friction, *f*, can be determined from the above equation if the values of σ_1 and σ_3 for reinforced soil and angle of internal friction, ϕ', for the unreinforced soil are known. Prediction charts for finding, *f*, values are presented in Figure 7 and Figure 8. From the charts the interface friction can be determined if the values of failure ratio (σ'_1/σ'_3), number of reinforcement layers (*N*) and angle of internal friction (ϕ') for the soil composites are known. In this analysis, equal spacing of reinforcement layers was assumed.

The combined friction angle or equivalent angle of internal friction is one of the important factors which will play a vital role for the improvement of the shear strength of the reinforced

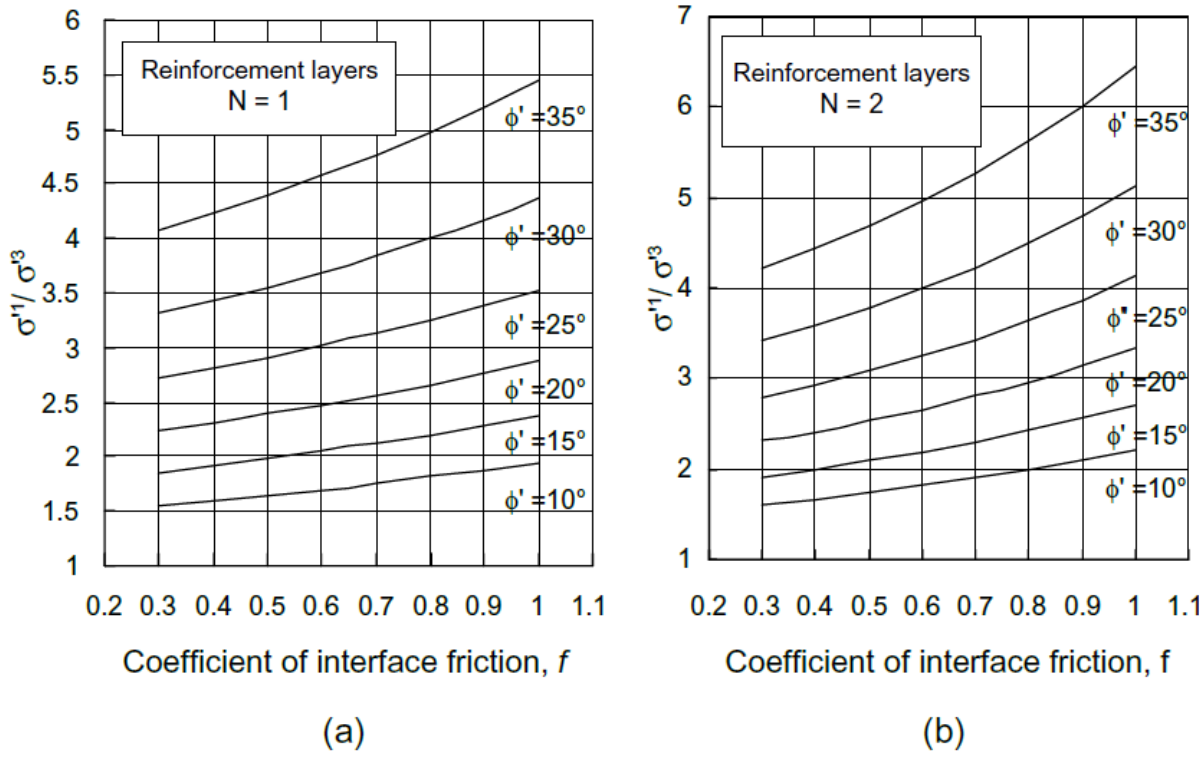

Figure 7. Prediction chart for the coefficient of interface friction for (a) single layer (b) two layer reinforced soil.

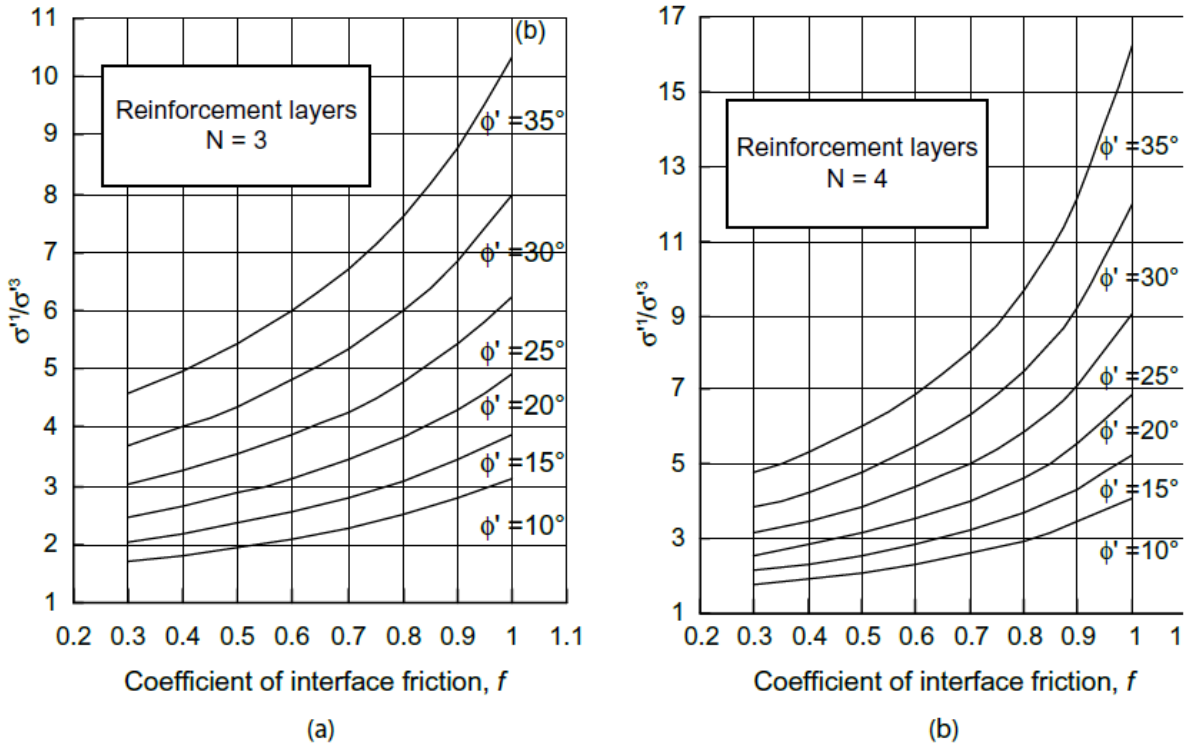

Figure 8. Prediction chart for the coefficient of interface friction for (a) three layer (b) four layer reinforced soil.

soil composites. For the evaluation of the equivalent friction angle, first a relation between the axial stress and confining stress at failure is written down as

$$\sigma_1 = \sigma_3 N_{\phi com} + 2c' \sqrt{N_{\phi com}}$$

where $N_{\phi com} = \tan^2(45 + \phi_{com}/2)$ in which ϕ'_{com} is the combined effective friction angle of reinforced soil. Expanding Equation 6 and rearranging, the combined angle of internal friction of reinforced soil can be determined as:

$$\tan^2(45+\phi'_{com}/2) = \frac{\tan^2(45+\phi'/2)}{\left[1-\frac{f\,d\,K_{av}}{2hK_a}\sum\left(1-\frac{2s}{h}\right)\right]}$$

8 CONCLUSIONS

Analytical relations are suggested to predict initial tangent modulus under various stress paths. The initial tangent moduli of unreinforced and reinforced soils are highly stress path dependent. Simplified approaches have been proposed for CTC stress paths to simulate the failure stress of the reinforced soil composites. Predictions of the shear strength of reinforced soils can be determined if the angle of internal friction of soil, numbers of reinforcement layer and interface friction coefficient are known. Prediction charts for obtaining the strength of reinforced soil and the coefficient of interface friction are given. A procedure for estimating the combined or equivalent friction angle from triaxial tests data is also presented.

REFERENCES

Ashmawy, A.K., Bourdeau, P.L., Drnevich, V.P. & Dysli, M. 1999. Cyclic response of geotextile-reinforced soil. Soils and Foundations, 39(1): 43–52.

ASTM 2000. Testing of geotextiles and related products. Annual Book of ASTM standards, 04.08. D4595.

Boscardin, M.D., Selig, E.T., Lin, R.S. & Yang, G.R. 1990. Hyperbolic parameters for compacted soils. *Journal of Geotechnical Engineering, ASCE,* 116(1): 89–103.

Broms, B.B. 1977. Triaxial tests with fabric-reinforced soil. Proc. Int. Conf. on the use of Fabrics in Geotechnics, Paris, France, 3: 129–133.

Chandrasekaran, B., Broms, B.B. & Wong, K.S. 1989. Strength of fabric reinforced sand under axisymmetric loading. Geotextiles and Geomembranes, 8: 293–310.

Cui, Y.J. & Delage, P. 1996. Yielding and plastic behaviour of an unsaturated compacted silt. *Geotechnique*, 46(2): 291–311.

Duncan, J.M., Byrne, P., Wong, K.S. & Mabry, P. 1980. Strength, stress-strain and bulk modulus parameters for finite element analysis of stresses and movements in soil. Geotechnical Engineering Research Report: UCB/GT/80–01, Department of Civil Engineering, University of California, Berkeley.

Ling, H.I. & Tatsuoka, F. 1992. Nonlinear analysis of reinforced soil structures by modified CANDE (M-CANDE) Geosynthetic-Reinforced Soil Retaining Walls, Jonathan Wu, (ed), 279–296. Rotterdam: Balkema.

Ling, H.I. & Tatsuoka, F. 1994. Performance of anisotropic geosynthetic-reinforced cohesive soil mass. Journal of Geotechnical Engineering, ASCE, 120(7): 1167–1184.

Taha, M.R, Mofiz, S.A. & Hossain, M.K. 1999. Behaviour of georeinforced residual soil in triaxial test. Proc. World Engineering Congress 99-Towards Engineering Vision: *Global Challenges and Issues*, 19th –22nd July, 1999, Kuala Lumpur, 175–180.

Yang, H. 1972. Strength deformation characteristics of reinforced sand. PhD Dissertation, University of California, Los Angeles, California.